

Asymptotic Approach for Rectangular Microstrip Patch antenna With Magnetic Anisotropy and Chiral Substrate

Zebiri Chemseddine, and Benabdelaziz Fatiha

Abstract—The effect of a chiral bianisotropic substrate on the complex resonant frequency of a rectangular microstrip resonator has been studied on the basis of the integral equation formulation. The analysis is based on numerical resolution of the integral equation using Galerkin procedure for moment method in the spectral domain. This work aim first to study the effect of the chirality of a bianisotropic substrate upon the resonant frequency and the half power bandwidth, second the effect of a magnetic anisotropy via an asymptotic approach for very weak substrate upon the resonant frequency and the half power bandwidth has been investigated. The obtained results are compared with previously published work [11-9], they were in good agreement.

Keywords—Microstrip antenna, bianisotropic media, resonant frequency, moment method.

I. INTRODUCTION

THE microstrip resonators appeared during the fifties, and they were especially developed during the seventies [1] [2]. They have small size, simplicity, easy manufacturing easy handle, besides they adjust easily to planar and non planar surfaces, and they present a big hardness when they are fixed on rigid surfaces. They are also very effective in terms of resonance, of polarization, of input impedance and radiations patterns [3] [4] [5].

The Major disadvantages of the microstrip resonators are in their weak purity of polarization, a narrow half-power bandwidth is typically in bout few percent. However, when increasing the substrate thickness, and reduction of the relative permittivity, there are techniques which can improve the resonator output until 90% by reducing the surface waves, and enable also an increase of the half-power bandwidth until 35% [6].

The resonant frequency of the microstrip resonator has been always strongly related to the dielectric of the substrate, and remains a very important factor to determine in resonator design. Some works have mentioned that a lot of uniaxial anisotropic substrate has been used for printed circuit resonator [7] [8].

However, studies concerning the resonant frequency calculation of the microstrip resonator, implemented on a

substrate of uniaxial anisotropy [9], have shown that this kind of substrate does not present any effect on the quality factor, the half-power bandwidth and obviously the resonant frequency. For these raisons other studies have been oriented on the cases of positive and negative anisotropy [9-11], or bi-anisotropic medium [12].

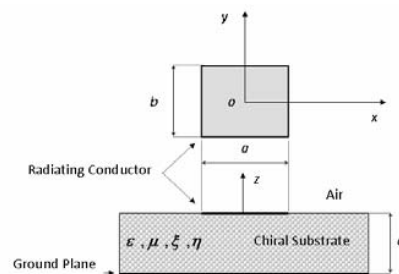


Fig. 1 Rectangular Microstrip Patch Antenna with Chiral substrate

In this paper the spectral approach (SDA) is used, this is intensively used in the analysis and design of planar structures. In such approach the tonsorial Green's spectral function which relates the tangential electric field components and the respective current of different conductor have to be determined. A great a mount of techniques have been used to evaluate this function [9]-[11] [13]-[17].

II. THEORY

A. Maxwell Equations

Composite chiral Materials which exhibit the effect of chirality at microwave frequencies have been fabricated and characterized in many studies [18],[19]. The chirals mediums considered here have a non homogenous gyroelectric (Fig. 1), they can be described by a set of constitutive relations [20].

$$\vec{B} = \vec{\mu}\vec{H} + \frac{1}{c_0}\vec{\xi}\vec{E} \quad (1)$$

$$\vec{D} = \vec{\epsilon}\vec{E} + \frac{1}{c_0}\vec{\eta}\vec{H} \quad (2)$$

where the permittivity and permeability tensors are of

C. Zebiri is with the Electrical Engineering Department, Ferhat Abbas University, Setif, 19000 Algeria (e-mail: zebiri@gmail.com).

F. Benabdelaziz is with the Electrical Engineering Department, Mentouti University, Constantine, 25000 Algeria (e-mail: benabdelaziz2003@yahoo.fr).

uniaxial anisotropy and the magneto-electric elements are respectively expressed as:

$$\bar{\mu} = \begin{bmatrix} \mu_t & 0 & 0 \\ 0 & \mu_t & 0 \\ 0 & 0 & \mu_z \end{bmatrix}, \bar{\varepsilon} = \begin{bmatrix} \varepsilon_t & 0 & 0 \\ 0 & \varepsilon_t & 0 \\ 0 & 0 & \varepsilon_z \end{bmatrix}, \text{ and} \quad (3)$$

$$\bar{\xi} = -\bar{\eta} = j \begin{bmatrix} 0 & \xi & 0 \\ -\xi & 0 & 0 \\ 0 & 0 & 0 \end{bmatrix}$$

Assuming an $e^{i\omega t}$ time variation and starting from Maxwell's equation in Fourier domain, we can show that the transverse fields in the chiral medium are expressed with respect to the longitudinal components \tilde{E}_z and \tilde{H}_z according to the following matrix equations:

$$\begin{aligned} \begin{bmatrix} \tilde{E}_x \\ \tilde{E}_y \end{bmatrix} &= \frac{1}{\kappa_s} \bar{F}(\bar{\kappa}_s) \begin{bmatrix} \tilde{E}_z \\ \tilde{H}_z \end{bmatrix} \\ &= \begin{bmatrix} j \frac{\varepsilon_z}{\varepsilon_t} \frac{1}{\kappa_s} \left(\kappa_0 \xi + \frac{\partial}{\partial z} \right) & 0 \\ 0 & \omega \frac{1}{\kappa_s} \mu_0 \mu_z \end{bmatrix} \begin{bmatrix} \tilde{E}_z \\ \tilde{H}_z \end{bmatrix} \end{aligned} \quad (4)$$

$$\begin{aligned} \begin{bmatrix} \tilde{H}_x \\ \tilde{H}_y \end{bmatrix} &= \frac{1}{\kappa_s} \bar{F}(\bar{\kappa}_s) \begin{bmatrix} \tilde{H}_z \\ -\tilde{E}_z \end{bmatrix} \\ &= \begin{bmatrix} \omega \frac{1}{\kappa_s} \varepsilon_0 \varepsilon_z & 0 \\ 0 & j \frac{\mu_z}{\mu_t} \frac{1}{\kappa_s} \left(\kappa_0 \xi + \frac{\partial}{\partial z} \right) \end{bmatrix} \begin{bmatrix} \tilde{E}_z \\ \tilde{H}_z \end{bmatrix} \end{aligned} \quad (5)$$

$$\text{with: } \bar{F}(\bar{\kappa}_s) = \begin{bmatrix} \kappa_x & \kappa_y \\ \kappa_y & -\kappa_x \end{bmatrix}, \quad \bar{\kappa}_s = k_x \hat{x} + k_y \hat{y} \quad (6)$$

where, $\bar{F}(\bar{\kappa}_s)$ is the kernel of the vector transforms, the superscripts e and h in (4) and (5) denote the TM and TE waves respectively, \tilde{E}_s and \tilde{H}_s are expressed According to the TE and TM modes.

Please submit your manuscript electronically for review as e-mail attachments. When you submit your initial full paper version, prepare it in two-column format, including figures and tables.

B. Transverse and Longitudinal Components

Taking into account the wave equation solution, we express the longitudinal components of the electric and magnetic field in the chiral medium according to the following expressions:

$$\tilde{E}_z(\kappa_s, z) = A^e e^{j\kappa_z^e z} + B^e e^{-j\kappa_z^e z} \quad (7)$$

$$\tilde{H}_z(\kappa_s, z) = A^h e^{j\kappa_z^h z} + B^h e^{-j\kappa_z^h z} \quad (8)$$

with,

$$\kappa_z^{e2} = \kappa_0^2 (\varepsilon_t \mu_t - \xi^2) - \frac{\varepsilon_t}{\varepsilon_z} \kappa_s^2 \quad (9)$$

$$\kappa_z^{h2} = \kappa_0^2 (\varepsilon_t \mu_t - \xi^2) - \frac{\mu_t}{\mu_z} \kappa_s^2 \quad (10)$$

where the spectral coefficients A^e, A^h, B^e and B^h are function of the variables κ_s, κ_z^e and κ_z^h , these are respectively the free space propagation for TE and TM modes. According to the previous equations, the following tangential components of the fields are obtained:

$$\tilde{E}_s(\kappa_s, z) = e^{j\bar{\kappa}_z z} \bar{A}(\kappa_s) + e^{-j\bar{\kappa}_z z} \bar{B}(\kappa_s) \quad (11)$$

$$\tilde{H}_s(\kappa_s, z) = e^{j\bar{\kappa}_z z} \bar{g}(\kappa_s) \bar{A}(\kappa_s) + e^{-j\bar{\kappa}_z z} \bar{h}(\kappa_s) \bar{B}(\kappa_s) \quad (12)$$

where,

$$\bar{\kappa}_z = \text{diag}[\kappa_z^e \quad \kappa_z^h] \quad (13)$$

$$\bar{A}(\kappa_s) = \left[j \frac{(-\kappa_0 \xi + j\kappa_z^e) \varepsilon_z}{\kappa_s^2} A^e \quad \frac{1}{\kappa_s^2} \omega \mu_0 \mu_z A^h \right]^T \quad (14)$$

$$\bar{B}(\kappa_s) = \left[j \frac{(-\kappa_0 \xi + j\kappa_z^e) \varepsilon_z}{\kappa_s^2} B^e \quad \frac{1}{\kappa_s^2} \omega \mu_0 \mu_z B^h \right]^T \quad (15)$$

$$\bar{g}(\kappa_s) = \text{diag} \left[\frac{\omega \varepsilon_0 \varepsilon_t}{j(-\kappa_0 \xi + j\kappa_z^e)} \quad \frac{j(\kappa_0 \xi + j\kappa_z^h)}{\omega \mu_0 \mu_t} \right] \quad (16)$$

$$\bar{h}(\kappa_s) = \text{diag} \left[\frac{\omega \varepsilon_0 \varepsilon_t}{j(-\kappa_0 \xi - j\kappa_z^e)} \quad \frac{j(\kappa_0 \xi - j\kappa_z^h)}{\omega \mu_0 \mu_t} \right] \quad (17)$$

For an electric and non magnetic medium having biaxial anisotropy with regard to the permittivity the previous expressions are well detailed in [11].

III. GREEN'S TENSOR EVALUATION

The proposed structure is studied and the boundary conditions have been applied after then the dyadic Green's function is obtained, this is expressed in compact form for transversal components as the following tensor:

$$\overline{\mathbf{G}}(\mathbf{k}_s) = \frac{\sin(\overline{\kappa}_z d)}{j\omega\epsilon_0} \text{diag} \left[\frac{N^e}{D^e} \kappa_z \kappa_z^e, \frac{1}{D^h} \kappa_0^2 \mu_t \right] \quad (18)$$

where,

$$N^e = \frac{1}{\kappa_z^e} \left(\kappa_0^2 \epsilon_t \mu_t - \frac{\epsilon_t}{\epsilon_z} \kappa_s^2 \right) \quad (19)$$

$$D^e = \epsilon_t \left(\kappa_z^e \kappa_z \cos(\kappa_z^h d) + j \left(\kappa_0^2 \mu_t - \frac{1}{\epsilon_z} \kappa_s^2 - j \kappa_z \kappa_0^2 \xi \right) \sin(\kappa_z^e d) \right) \quad (20)$$

$$D^h = \kappa_z^h \cos(\kappa_z^h d) + j \left(\kappa_z \mu_t - j \kappa_0^2 \xi \right) \sin(\kappa_z^h d) \quad (21)$$

IV. INTEGRAL EQUATION SOLUTION

The integral equation describing the electric field on the patch is expressed by application of the boundary condition on tangential components [9]-[11] as:

$$\int_{-\infty}^{\infty} d\kappa_s \overline{\mathbf{F}}(\overline{\kappa}_s) \cdot \overline{\mathbf{G}}(\kappa_s) \cdot \tilde{\mathbf{J}}(\kappa_s) = 0 \quad (22)$$

Using the Galerkin procedure of the moment method in Fourier domain, enable the integral equation in (22) to be discretized into matrix equation. Where the currents surfaces \mathbf{J} on the plate are expanded into a finite series of basis function J_{xn} and J_{ym} according to the following expression:

$$\mathbf{J}(r_s) = \sum_{n=1}^N a_n \begin{bmatrix} J_{xn}(r_s) \\ 0 \end{bmatrix} + \sum_{m=1}^M b_m \begin{bmatrix} 0 \\ J_{ym}(r_s) \end{bmatrix} \quad (23)$$

where, a_n and b_m are the mode expansion coefficients to be sought. We Substitute the vector Fourier transform of (23) into (22). Subsequently, the resulting equation is tested by the same set of basis functions that was used in the expansion of the patch current. Thus, the integral equation (22) is brought into the following matrix equation:

$$\begin{bmatrix} \overline{\mathbf{B}}_1 \\ \overline{\mathbf{B}}_3 \end{bmatrix}_{N \times N} \begin{bmatrix} \overline{\mathbf{B}}_2 \\ \overline{\mathbf{B}}_4 \end{bmatrix}_{N \times M} \cdot \begin{bmatrix} (a)_{N \times 1} \\ (b)_{M \times 1} \end{bmatrix} = 0 \quad (24)$$

where, $(\overline{\mathbf{B}}_i)_{j \times k}$ are the elements of the digitalized matrix equation.

A. Resonant Frequency and Half Power Bandwidth

Equation (24) has a non trivial solution only in the case where the condition below is verified.

$$\det(\overline{\mathbf{B}}(\omega)) = 0 \quad (25)$$

The resonator is designed to operate near its resonant frequency, and all its characteristics are estimated around this frequency, for this reason equation (25) is called characteristic equation for the complex resonant frequency $f = f_r + jf_i$, where f_r : is the resonant frequency and f_i : point to losses by radiation in the case of radiating antenna, the quality factor and the half power bandwidth are defined in [21] [22] as:

$$Q = f_r / (2f_i) \quad (26)$$

$$BW = 1/Q \quad (27)$$

B. Effect of the Anisotropic Substrate

The effect of the two chiral's constitutive parameters has been studied, which are: the chirality and the magnetic uniaxial anisotropy of the substrate upon the complex resonant frequency and the half power bandwidth of the microstrip resonator. In order to make validation of the results obtained a comparison with the isotropic dielectric case presented in the literature.

The figures presented below show the Normalized real and imaginary part of the resonant frequency, as well as the half power bandwidth width respect to the bi-anisotropic substrate thickness of a microstrip structure without shielded layer, compared to measures in the literature with ($\epsilon_s = \epsilon_c = 2.35$ and $\epsilon_s = \epsilon_c = 7$), the considered medium is defined as follow:

$\eta = \xi = -1, 0$ and 1 respectively (Magneto-electric elements), ($\mu_t = 0.8, \mu_z = 1$) (Positive anisotropy of the permeability), ($\mu_t = 1.2, \mu_z = 1$) (Negative anisotropy). The uniaxial anisotropy is obtained by changing μ_t and keeping μ_z constant.

To put in evidence the effect of the constitutive parameters of the dielectric chiral layer, we can consider the asymptotic form of the resonant frequency, when the layer d is electrically weak. However the dyadic Green's function takes the following form.

$$\overline{\mathbf{G}}(\mathbf{k}_s) \xrightarrow{d \rightarrow 0} \frac{d}{j\omega\epsilon} \text{diag} \left[\kappa_0^2 \mu_t - \frac{1}{\epsilon_z} \kappa_s^2, \mu_t \kappa_0^2 \right] \quad (28)$$

Some authors such as Chew [10], have shown that only one basis function ($N=0, M=1$) is function is needed to obtain excellent convergence of results. In this case the current distribution on the patch conductor is given by:

$$\mathbf{J}(\mathbf{r}_s) = b_1 \begin{bmatrix} 0 \\ \sin \left[\frac{\pi}{b} \left(y + \frac{b}{2} \right) \right] \end{bmatrix} \quad (29)$$

And the characteristic equation for the resonant frequency driven from the fourth element of the matrix equation (24) is given as:

$$(\overline{\mathbf{B}}_4) = \int_{-\infty}^{+\infty} d\kappa_s \left[\kappa_0^2 \mu_t - \frac{1}{\epsilon_z} \kappa_y^2 \right] \tilde{J}_{y1}(-\kappa_s) \tilde{J}_{y1}(\kappa_s) = 0 \quad (30)$$

The function J_{y1} has a Fourier transform given by the analytical expression:

$$\tilde{J}_{y1}(\kappa_s) = \pi b \frac{\sin(\kappa_x \frac{a}{2}) \cos(\kappa_y \frac{b}{2})}{\kappa_x \left[\left(\frac{\pi}{2} \right)^2 - \left(\kappa_y \frac{b}{2} \right)^2 \right]} \quad (31)$$

Using the asymptotic expression of $\bar{\mathbf{G}}$ given by (28) and taking into account (31), the equation (30) becomes:

$$\kappa_0^2 \mu_t I_1 - \frac{4}{\varepsilon_z b^2} I_2 = 0 \quad (32)$$

where,

$$I_1 = \int_0^\infty d\kappa_y \frac{\cos^2 \kappa_y}{\left[\kappa_y^2 - (\pi/2)^2 \right]^2}, \quad I_2 = \int_0^\infty d\kappa_y \frac{\kappa_y^2 \cos^2 \kappa_y}{\left[\kappa_y^2 - (\pi/2)^2 \right]^2} \quad (33)$$

Using the Integration along the Contour of the spectral domain, the integral equations of (33) is resolved analytically

$$\text{as: } I_1 = \frac{1}{\pi}, \text{ and } I_2 = \frac{\pi}{4} \quad (34)$$

Substituting (34) into (32) we will get estimation of the resonant frequency, expressed by:

$$f_r = \frac{c}{2b\sqrt{\varepsilon_z \mu_t}} \quad (35)$$

where, c is the light speed in the vacuum. The resulting formula gives an idea on the effect of the parameters ε_z and μ_t upon the antenna resonant frequency. It is clear that this latter depend on the permittivity along the optic axis and the perpendicular component of the permeability in the limit of weak substrate. We can for this kind of resonator improve their performances by treating only the components ε_z and μ_t .

V. NUMERICAL ANALYSIS

The dielectric medium provided with chirality and magnetic uniaxial anisotropy is studied, and the effect upon the complex resonant frequency and the half-power bandwidth has been observed. The substrate is considered to be bi-anisotropic with relative permittivity such as: $\varepsilon_x = \varepsilon_z = 7$ and $\varepsilon_y = \varepsilon_z = 2.35$. The dimensions of the rectangular patch are 1 cm, 1.5 cm. In Fig. 2, the complex resonant frequency and the half power bandwidth are presented with respect to the substrate thickness and for different values of chirality and depending on the magnetic anisotropy choice. The normalization is presented with respect to the frequency f_0 which is obtained from the fundamental mode $f_r = c / 2b\sqrt{\varepsilon_z}$.

Numerical results presented by the Figs. 2-3, show that positives values of chirality, lead to an increase in the real part of the resonant frequency and a reduction in the imaginary part, which lead to a considerable reduction in half power bandwidth according to an increase in the thickness of the

chiral layer, and inversely for the case of negative value of chirality. These obtained characteristics are required in the design of cavities, oscillators and filters for hyper-frequency application, according to their required properties.

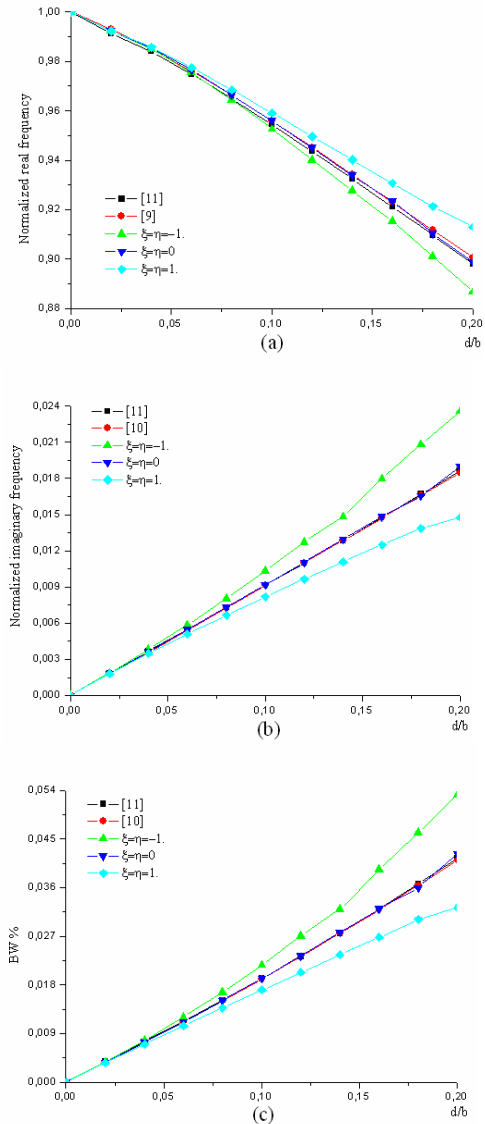


Fig. 2 Normalized resonant frequency, $a=1.5\text{cm}$, $b=1\text{cm}$, $\varepsilon_r=7$ (a) real part (b) imaginary part (c) Half-power bandwidth

On the other hand, for small thickness, the half power bandwidth remains slightly sensitive to the effect of the magneto-electric element. This result can also be verified by the asymptotic formula. Whereas for the same value of chirality, but for different values of permittivity, the increase of the real part of the resonant frequency and the diminution of imaginary part, lead to a diminution in the half power bandwidth and an increase of the quality factor.

And for the case of $\varepsilon_x = \varepsilon_z = 2.35$, and the one: $\varepsilon_x = \varepsilon_z = 7$, our notices remain the same as the case of negative chirality, which means for $\varepsilon_x = \varepsilon_z = 2.35$, the real part of the resonant

frequency increase and the imaginary part decrease to much compared to other cases. Consequently, for resonators implemented on chiral it is very imperative to use relatively small permittivity constant for the advantages stated in the literatures [6].

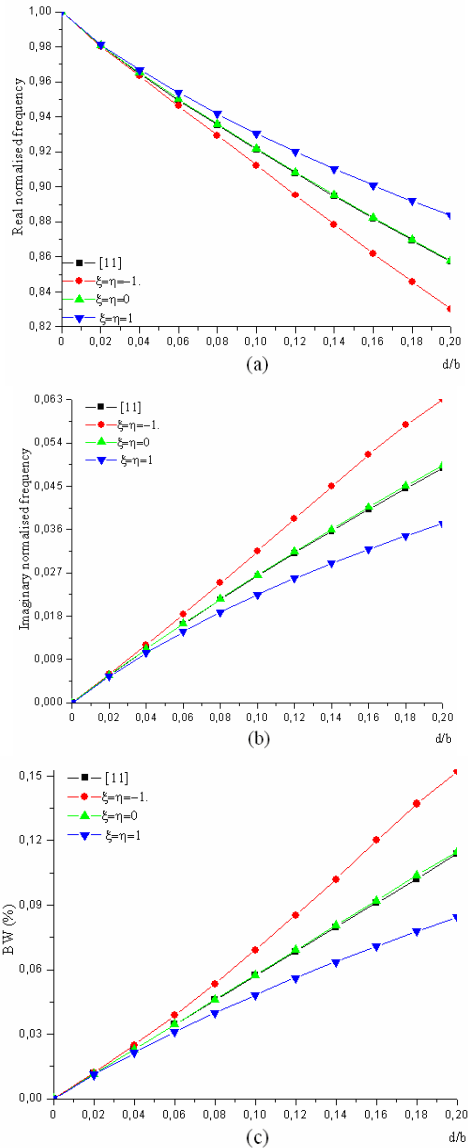


Fig. 3 Normalized resonant frequency, $a=1.5\text{cm}$, $b=1\text{cm}$, $\epsilon_r=2.35$ (a) real part (b) imaginary part (c) Half-power bandwidth

We notice that in the chiral substrate, an increase in the real part of the resonant frequency (case of the positive magneto-electric element). The same is for the imaginary part (case of the negative magneto-electric element) whereas for the case of isotropic substrate, to obtain such values of frequencies, one has to use miniature structure.

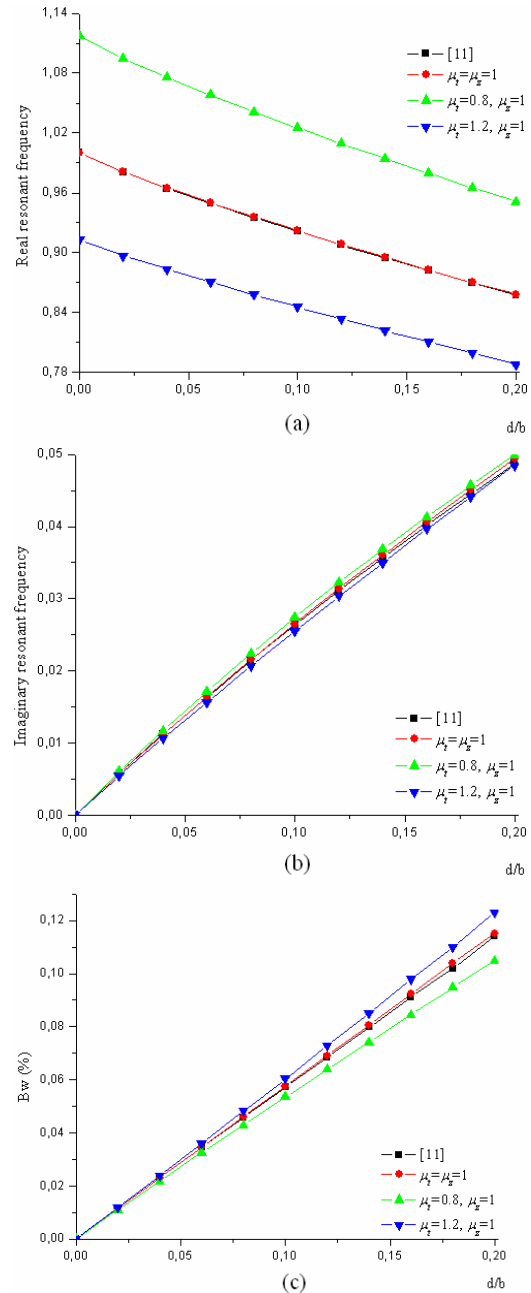


Fig. 4 Normalized resonant frequency, $a=1.5\text{cm}$, $b=1\text{cm}$, $\epsilon_r=2.35$ (a) real part (b) imaginary part (c) Half-power bandwidth

The Fig. 4, show a notable effect of the axial anisotropy of the permeability upon the real resonant frequency, as shown by the asymptotic formula. Whereas for the imaginary part and the half power bandwidth, we notice that this effect is slightly similar to the effect of the uniaxial anisotropy of the permittivity. We can use this effect in the case of a test for diminution or increase of the resonant frequency without changing the imaginary part or the half power bandwidth.

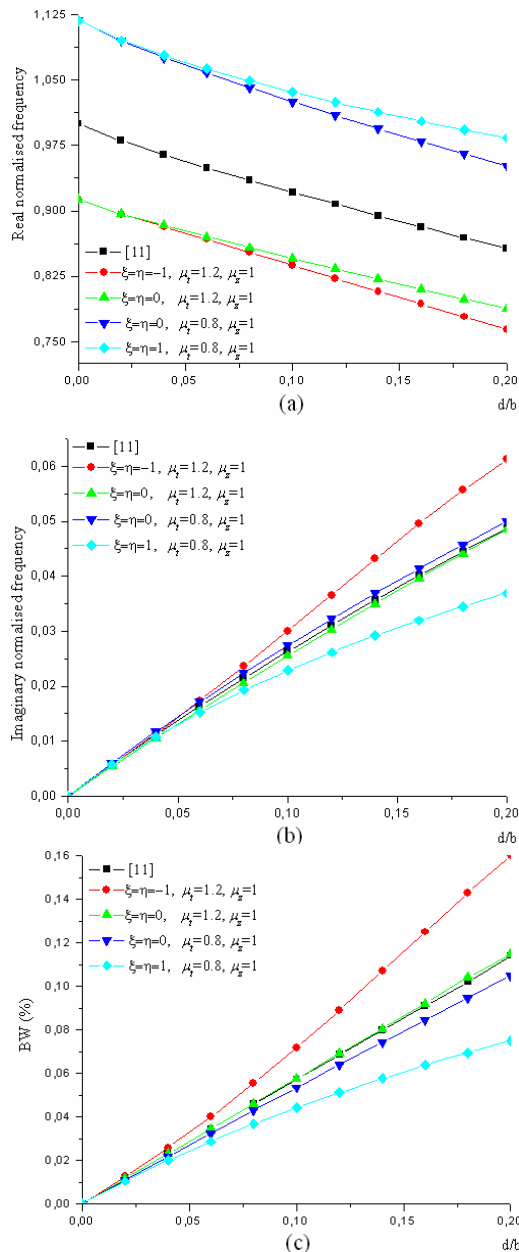


Fig. 5 Normalized resonant frequency, $a=1.5\text{cm}$, $b=1\text{cm}$, $\epsilon_r=2.35$ (a) real part (b) imaginary part (c) Half-power bandwidth

The Fig. 5, show the extreme effects of the constitutive parameters such as: chirality magnetic uniaxial anisotropy. We can use these advantageous properties in the resonators design where the use of permittivity affects directly the real frequency and slightly the imaginary part (in the same way for increase as for decrease). But the chiral substrate reverse this way of effect, an increase of one complex part incites the diminution of the other part, which offers a wide interval for the resonant frequency.

VI. CONCLUSION

According to the literature, the positive uniaxial anisotropy introduces a slight increase in the half-power bandwidth, while this latter is subject to a slight diminution for negative uniaxial anisotropy. Whereas in our case the structure is implemented in a chiral substrate, the results show that the effect of the constitutive parameters (chirality, permeability) is very apparent on the half-power bandwidth and the resonant frequency, according to the choice of the chirality element: the positive case presents a diminution of the real part of the resonant frequency and an increase of the imaginary part. The inverse is obtained for the negative case of chirality. The advantage of the uniaxial anisotropy of the permeability is on the widening of the half-power bandwidth which can be very important for a radiating cavity application; the inverse is obtained for the case of cavity built for filter use.

The introduction of the chiral as substrate leads to various applications. Its main effect is the ability of structure miniaturization, which makes easy electronics components integration.

REFERENCES

- [1] Constantine A. Balanis, "Antenna Theory: Analysis and Design", 2ième Edition, pp. 722-783, John Wiley & Sons, Inc., New York, 1997.
- [2] G. A. Deschamps, "Microstrip Microwave Antennas", present to the third Symposium over the resonators, 1953.
- [3] W. F. Richards, Y. T. Lo et D. D. Harrison, "An Improved Theory of Microstrip Antennas with Applications", IEEE Trans. Antennas Propagat., Vol. AP-29, No. 1, pp. 38-46, Jan. 1981.
- [4] D. H. Schaubert, F. G. Farrar, A. Sindoris, and S. T. Hayes, "Microstrip Antennas with Frequency Agility and Polarisation Diversity", IEEE Trans. Antennas Propagat., Vol. AP-29, No. 1, pp. 118-123, Jan. 1981.
- [5] M. P. Purchine et J. T. Aberle, "A Tunable L-Band Circular Microstrip Patch Antenna", Microwave Journal, pp. 80, 84, 87 et 88, Oct. 1994.
- [6] D. M. Pozar, "Microstrip Antennas", Proc. IEEE, Vol. 80, No. 1, pp. 79-81, Jan. 1992.
- [7] N. G. Alexopoulos, "Integrated-circuit structures on anisotropic substrate," IEEE Trans. Microwave Theory Tech., vol. MTT-33, pp. 847-881, Oct. 1985.
- [8] D. M. Pozar, "Radiation and scattering from a microstrip patch on a uniaxial substrate", IEEE Trans. Antennas Propagat., vol. AP-35, pp. 613-621, June 1987.
- [9] Kin-Lu Wong, Jeen-Sheen Row, Chih-Wen Kuo, and Kuang-Chih Huang "Resonance of a Rectangular Microstrip Patch on a Uniaxial Substrate". IEEE Trans. Microwave Theory and Techniques, vol. 41, pp. 698-701, April 1993.
- [10] W. C. Chew and Q. Liu, "Correction to "Resonance frequency of a rectangular microstrip patch" " IEEE Trans. Antennas Propagat., vol. 36, pp. 1827, Dec. 1988.
- [11] F. Boutout, F. Benabdelaziz, T. Fortaki and D. Khedrouche, "Resonant frequency and bandwidth of a superstrate-loaded rectangular patch on a uniaxial anisotropic substrate," Communications in Numerical Methods in Engineering (John Wiley & Sons), vol. 16, issue : 7, pp. 459-473, July 2000.
- [12] Filiberto Bilotti and Lucio Vegni, "Chiral Cover Effects on Microstrip Antennas", IEEE Transactions On Antennas And Propagation, vol. 51, no. 10, October 2003. pp2891.
- [13] T. Itoh, "Spectral domain immittance approach for dispersion characteristics of generalized printed transmission lines," IEEE Trans. Microwave Theory Tech., vol. MTT-28, pp. 733-736, July 1980.
- [14] N. K. Das and D. M. Pozar, "A generalized spectral-domain Green's function for multilayer dielectric substrates with application to multilayer transmission lines," IEEE Trans. Microwave Theory Tech., vol. MTT-35, pp. 326-335, March 1987.
- [15] F. L. Mesa, R. Marques, and M. Horno, "A general algorithm for computing the bidimensional spectral Green's dyad in multilayered

- complex bianisotropic media: The equivalent boundary method", IEEE Tran. Microwave Theory Tech., vol. 39, pp. 1640-1649, 1991.
- [16] P. Bernardi and R. Cicchetti, "Dyadic Green's function for conductor-backed layered structures excited by arbitrary tridimensional sources", IEEE Trans. Microwave Theory Tech., vol. 42, pp. 1474-1483, 1994.
- [17] A. Dreher, "A new approach to dyadic Green's function in spectral domain" IEEE Trans. Antennas Propagat., vol. 43, pp. 1297-1302, Nov. 1995.
- [18] K. W. WHITES, CHUNG C. Y., "Composite uniaxial bianisotropic chiral materials characterization: Comparison of predicted and measured scattering", Journal of electromagnetic waves and applications, vol. 11, pp. 371-394, 1997.
- [19] G. Busse, J. Reinert, and, A. F. Jacob, "Waveguide Characterization of Chiral Material: Experiments" IEEE Transactions on Microwave Theory And Techniques, vol. 47, pp. 297-301, 1999.
- [20] V. Dmitriev; "Tables Of The Second Rank Constitutive Tensors For Linear Homogeneous Media Described By The Point Magnetic Groups Of Symmetry"; Progress In Electromagnetics Research, PIER 28, 43-95, 2000
- [21] D. M. Pozar, "General relations for a phased array of printed antennas derived from infinite current sheets," IEEE Trans. Antennas Propagat., vol. AP-33, pp. 498-504, May. 1985.
- [22] W. P. Harokopus, L. P. B. Katehi, W. Y. Ali-Ahmed, and G. M. Rebiez, "Surface wave excitation from open microstrip discontinuities," IEEE Trans. Microwave Theory Tech., vol. 39, pp. 1098-1107, July. 1991.